Inflammatory responses of a human keratinocyte cell line to 10 nm citrate- and PEG-coated silver nanoparticles

Bastos V.[1], Brown D.[2], Johnston H. [2], Daniel-da-Silva, A.L. [3], Duarte I.F. [3], Santos C. [1,4] and Oliveira H.[1]

[1]*CESAM & Laboratory of Biotechnology and Cytomics, University of Aveiro, 3810-193 Aveiro, Portugal*

[2]*School of Life sciences, Heriot-Watt University, Riccarton, Edinburgh EH14 4AS, UK*

[3]*CICECO – Aveiro Institute of Materials, Department of Chemistry, University of Aveiro, 3810-193 Aveiro, Portugal*

[4]*Department of Biology & Greenup / Citab -UP, Faculty of Sciences, University of Porto, Rua do Campo Alegre, Porto*

*corresponding author: csantos@fc.up.pt

Abstract

Silver nanoparticles (AgNPs) are among the most commonly used engineered NPs and various commercially available products are designed to come in direct contact with the skin (wound dressings, textiles, creams, among others). Currently, there is limited understanding of the influence of coatings on the toxicity of AgNPs and in particular their ability to impact on AgNP's mediated inflammatory responses. As AgNPs are often stabilized by different coatings, including citrate and polyethyleneglycol (PEG), in this study we investigate the influence of citrate (Cit10) or PEG (PEG10) coatings to 10 nm AgNP on skin, using human HaCaT keratinocytes. AgNPs cytotoxicity and inflammatory response (nuclear factor (NF)-κB induction and cytokine production) of HaCaT were assessed after *in vitro* exposure to 10 μg/mL and 40 μg/mL after 4, 24 and 48 h. Results showed that although both types of coated AgNPs decreased cell proliferation and viability, Cit10 AgNPs were more toxic. NF-κB inhibition was observed for the highest concentration (40 μg/mL) of PEG10 AgNPs, and the putative link to early apoptotic pathways observed in these cells is discussed. No production of IL-1β, IL-6, IL-10 and TNFα was stimulated by AgNPs. Furthermore, Cit10 and PEG10 AgNPs decreased the release of MCP-1 by HaCaT cells after 48 h of exposure. As cytokines are vital for the immunologic regulation in the human body, and it is demonstrated that they may interfere with NPs, more research is needed to understand how different AgNPs affect the immune system.

Introduction

Nanotechnology-based consumer products are exponentially increasing, being nanosilver-containing products among the most commonly used (Vance et al., 2015). Silver nanoparticles (AgNPs) are widely used due to their enhanced physicochemical properties and biological activities such as their antimicrobial activity. Their applications range from medicine and industry to household and personal care products (EPA, 2010) or clothing (Abdelhalim and Jarrar, 2011; Behra et al., 2013; Benn and Westerhoff, 2008; Eckhardt et al., 2013; Nowack et al., 2011). The increased exploitation of AgNPs and consequent release into the environment raises concerns about their possible impacts on the environment and on human health (Nowack and Bucheli, 2007). There is an array of AgNPs that are being exploited, which vary with respect to their physicochemical properties (e.g. size, shape, charge, surface coating, dispersion state) (Ahlberg et al., 2014; Boonkaew et al., 2014; Comfort et al., 2014; Kim et al., 2012; Park et al., 2011b). Existing studies have demonstrated that the physicochemical properties of AgNPs are able to influence their toxicity for different cell lines [eg., human keratinocytes (HaCaT and primary keratinocytes), normal fibroblasts (NHF), rat adrenal pheochromocytoma (PC12), and mouse osteoblasts (MC3T3-E1), fibroblasts (L929) and macrophages (RAW 264.7)]. However, little attention has been given to the coating-dependent toxicity of AgNPs. Thus, research on the

toxicity of AgNPs of varied physicochemical properties is critical in order to better predict the risks they pose.

It has been reported that nanoparticle coating, media composition and ionic strength influence the surface chemistry, shape, aggregation state and dissolution of AgNPs, which in turn can differently affect their cellular uptake and biological effects (Tejamaya et al., 2012). Indeed, a few studies addressing the uptake (by embryonic fibroblasts NIH/3T3, keratinocytes HaCaT and hepatoma cells Hepa-1c1c7, respectively) of different coated AgNPs and their influence on cytotoxicity have been reported (Caballero-Díaz et al., 2013; Lu et al., 2010; Pang et al., 2015). Citrate is the most commonly used reducing and stabilizing agent of AgNPs, rendering NPs with a negative surface charge and providing colloidal stability through electrostatic repulsions (Sharma et al., 2009). Among other coating agents of AgNPs, low molecular weight polyethyleneglycol (PEG), which stabilizes AgNPs through steric interactions, has been increasingly used in biomedical applications as it enhances biocompatibility and increases blood circulation time (Ginn et al., 2014; Ryan et al., 2008).

Assessment of the ability of NPs to induce inflammatory responses is commonly used as an indicator of toxicity. For example, Chalew and Schwab (2013) studied the inflammatory effects of AgNPs, titanium dioxide (TiO_2NPs), and zinc oxide (ZnONPs) (0, 0.1, 1, 10, and 100 mg/L) on human intestinal Caco-2 and SW480 cells and found that all NPs increased IL-8 cytokine generation in both cell lines. Also, Park et al (2011a) observed that pro-inflammatory cytokines (IL-1, TNF-α, and IL-6) and Th0 cytokine (IL-2) were progressively increased by day 28 after a single intratracheal instillation of AgNPs in mice. Suliman and co-workers (2013b) found that 50 µg/mL AgNPs exposure to human lung epithelial (A549) cells significantly increased the level of pro-inflammatory cytokines, namely interleukin-1β (IL-1β) and interleukin-6 (IL-6). Yang and collaborators also observed IL-1β release by human blood monocytes in response to AgNPs (Yang et al., 2012). However, Wong et al (2009) found an anti-inflammatory effect of AgNPs to two mouse macrophage cell lines, RAW264.7 and J774.1, where AgNPs blocked TNF-α production. On the other hand, we could not found studies reporting the induction of anti-inflammatory cytokines after exposure to NPs (Murray et al., 2013; Orlowski et al., 2013; Samberg et al., 2009). Cytokines can strongly activate inflammatory responses and cell death in various tissues, including the skin (Fujiwara and Kobayashi, 2005; Graves et al., 2004). Indeed, a study on the effects of UVB radiation using HaCaT cells reported an increase of various pro-inflammatory cytokines - interleukin (IL)-1β IL-6, IL-8, interferon (IFN)-γ, granulocyte-colony stimulating factor (G-CSF), macrophage inflammatory protein (MIP)-1β, and tumor necrosis factor (TNF)-α (Yoshizumi et al., 2008). Murray et al (2013) found increased IL-8 and IL-6 in human epidermal keratinocytes (HEK cells) after exposure to superparamagnetic iron oxide (SPION) NPs (2.6, 5.2, 13, and 26 µg/cm^2 for 24 h). In other study using HEK cells, quantum dot NPs significantly increase IL-6 at 1.25 nM to 10 nM, while IL-8 increased from 2.5 nM to 10nM

after 24 h and 48 h (Zhang et al., 2008). Therefore, as products containing AgNPs can be applied to the skin (e.g. wound dressing), and as there are experimental evidences for skin penetration of 25 ± 7 nm AgNPs (also in intact skin) (Larese et al., 2009) and 20 – 40 nm AgNPs (George et al., 2014), the human keratinocyte cell line HaCaT was selected as an *in vitro* model in this study. It is well known that cytokines play crucial roles in immunologic regulation in the human body and are involved in the induction of proliferation, differentiation, and cell death in many cell types (Yarilin and Belyakov, 2004). Moreover, activation of the transcription factor nuclear factor kappa B (NF-κB) has been shown to play a central role in the enhanced expression and regulation of cytokine genes (Kelso, 1998). There is also evidence that carbon NPs can activate NF-κB in macrophages which stimulates TNFα production (Brown et al., 2004). To our knowledge, the activation of NF-κB in keratinocytes has not been studied previously.

In our previous study (Bastos et al., 2016) we evaluated the toxicity of 30 nm AgNPs coated with citrate or PEG on HaCaT cells. Our results showed that Cit30 AgNPs were more cytotoxic than PEG30 AgNPs. Concerning cytokine release, both Cit30 and PEG30 AgNPs induced a decrease in MCP-1 production but no effect on other cytokines, namely IL-1β, IL-6, IL-10 and TNF-α (Bastos et al, 2016).

In this study, we aimed to compare the inflammatory responses of HaCaT cells exposed to well-characterized 10 nm AgNPs coated with citrate or PEG, in order to explore the influence of smaller sizes of AgNPs on the inflammatory response. In particular, the effects on viability, expression of the pro-inflammatory transcription factor NF-κB and production of cytokines such as interleukin-1 beta (IL-1β), IL-6, tumour necrosis factor-alpha (TNF-α), IL-10 and monocyte chemoattractant protein-1 (MCP-1) were assessed.

Material and methods

Chemicals

Sterile, purified and endotoxin-free silver nanoparticles (Biopure AgNPs 1.0 mg/mL in water), with a diameter of 10 nm and a citrate or polyethyleneglycol (PEG) surface, designated as Cit10 and PEG10, respectively, were purchased from Nanocomposix Europe (Prague, Czech Republic). Dulbecco's modified Eagle's medium (DMEM), fetal bovine serum (FBS), antibiotics and phosphate buffer saline (PBS, pH 7.4) were purchased from Life Technologies (Carlsbad, CA, USA). 3-(4,5-dimethylthiazol-2-yl)-2,5-diphenyltetrazolium bromide (MTT), Mowoil and DAPI were obtained from Sigma-Aldrich (St. Louis, MO, USA).

Physicochemical characterization of AgNPs

The morphology and size of AgNPs were assessed by transmission electron microscopy (TEM) using a transmission electron microscope Hitachi H9000 NAR (Hitachi High-Technologies Europe GmbH, Germany) operating at 300 kV. Samples for TEM analysis were prepared by

evaporating dilute suspensions of AgNPs on a copper grid coated with an amorphous carbon film. The hydrodynamic diameter and polydispersity index (PdI) were measured by dynamic light scattering (DLS) and the zeta potential was assessed by electrophoretic mobility, both measurements using a Zetasizer Nano ZS (Malvern Instruments, UK). Silver quantification measurements were performed by inductively coupled plasma optical emission spectrometry (ICP-OES) in an Activa M Radial spectrometer (Horiba Jobin Yvon), employing a charge coupled device (CCD) array detector, with a wavelength range of 166–847 nm and radial plasma view. Samples for ICP-OES were prepared by addition of 10 µL AgNPs (1.0 mg/mL) to 990 µL of either ultrapure water or complete culture medium, incubated for 0, 4, 24 or 48h, then centrifuged at 40000 rcf for 120 min at 4ºC (in accordance with the manufacturer's recommendations) to deposit the nanoparticles and separate the supernatant, which was then digested with acid (HCl:HNO_3 2:1 v/v) before ICP-OES analysis.

Cell Culture

The HaCaT cell line, a nontumorigenic immortalized human keratinocyte cell line (Boukamp et al., 1988), was obtained from Cell Lines Services (Eppelheim, Germany). Cells were grown in complete medium, i.e., Dulbecco's modified Eagle's medium, supplemented with 10% fetal bovine serum (FBS), 2 mM L-glutamine, 100 U/mL penicillin, 100 µg/mL streptomycin and 250 µg/mL fungizone at 37 °C in 5% CO_2 humidified atmosphere. Cells were observed daily under an inverted phase-contrast Eclipse TS100 microscope (Nikon, Tokyo, Japan). For each experiment, cells were allowed to adhere for 24 h and then exposed to Cit10 or PEG10 AgNPs (dispersed through vortex in cell culture medium). For the assays cells were in passage number 45-50. Depending on the experiment, the silver ion and the coating agent per se, dissolved in complete medium, were used as controls. The effects were measured after 4, 24 and 48 h.

Viability assay

Cell viability was determined by the colorimetric 3-(4,5- dimethyl-2-thiazolyl)-2,5-diphenyl tetrazolium bromide (MTT) assay, measuring intracellular reduction of tetrazolium salts into purple formazan by viable cells (Twentyman and Luscombe, 1987). Cells were seeded in 96-well plates at a concentration of $6x10^4$ cells/mL. Fifty microliters of MTT (1 mg/mL) in phosphate buffered saline (PBS) were then added to each well, and incubated for 4h at 37 °C, 5% CO_2. Medium was then removed and 150 µL of DMSO were added to each well for solubilization of formazan crystals. The optical density of reduced MTT was measured at 570 nm in a microtiter plate reader (Synergy HT Multi-Mode, BioTeK, Winooski, VT), and cell viability was calculated as [(Sample Abs –DMSO Abs) / (Control Abs – DMSO Abs)]*100. Three independent assays were performed with at least 2 technical replicates each and the results compared with the control (no exposure). From our previous MTT results (Bastos et al., 2016), the IC50 for 30 nm citrate

coated AgNPs (the most cytotoxic) was 40 mg/mL and 37.4 mg/mL at 24 and 48 h respectively. Therefore, the concentrations of AgNPs corresponding to IC50 and IC20 (40 mg/mL and 10 mg/mL, respectively) were selected for 10 nm AgNPs assays in order to enable comparisons between sizes.

Immunofluorescence of p65 subunit of NF-κB in human keratinocytes

After the 4 h treatments with 10 and 40 µg/mL of Cit10 or PEG 10AgNPs, coverslips were washed with PBS and permeabilized with 0.2% Triton X-100 for 15 min followed by three washes with PBS. Cells were treated with PBS containing BSA at a concentration of 1 mg/mL as a blocking agent for 1 hour. Cells were then washed three times with PBS and treated with anti-human NF-κB antibody (p65 subunit, Santa Cruz Biotechnology,Inc. Dallas, Texas USA) diluted 1/200 in PBS plus 0.5% BSA for 1 hour at room temperature. After three washes with PBS, coverslips were treated with a second antibody, Alexa fluor 488 anti-rabbit IgG diluted 1:200 in PBS plus 0.5% BSA for 1 hour at room temperature. After three washes with PBS, coverslips were treated with 0.5µg/ml DAPI in PBS plus 0.5% BSA for 20 seconds, washed in PBS and mounted on glass microscope slides using Mowoil. Cells were imaged using confocal microscopy.

Cytokine estimation using cytometric bead array

Cytokine production was assessed using Bioplex kits. Briefly, the supernatants (collected from cell viability studies, centrifuged and frozen at -80ºC) were used to estimate the release of the following cytokines from treated cells: interleukin-1 beta (IL-1β), IL-6, tumour necrosis factor-alpha (TNF-α), IL-10 and monocyte chemoattractant protein-1 (MCP-1). Bead array kits were obtained from Beckton Dickinson (Oxford, UK) and a master mix prepared according to the manufacturer's instructions. The master mix was incubated with each of the test supernatants for 1 h, followed by the addition of detection beads and incubated for a further 2 h at room temperature. The beads were then washed in wash buffer and analysed using a BD FACSArray™ flow cytometer which had previously been set up and calibrated using standard beads for each cytokine under investigation.

Statistical analysis

The results are reported as mean ± standard deviation (SD) of 2 technical replicates in each of the 3 independent experiments. For MTT assay, the statistical significance between control and exposed cells was performed by one-way ANOVA, followed by Dunnet and Dunn's method (as parametric and non-parametric test, respectively), using Sigma Plot 12.5 software (Systat Software Inc.). For the other assays, results were compared using two-way ANOVA, followed by Holm-Sidak test using also Sigma Plot 12.5 software (Systat Software Inc.). The differences were considered statistically significant for $p < 0.05$.

Results

Physicochemical characterization of AgNPs

A summary of the physico-chemical properties of the NMs is provided in table 1. The spherical shape and diameter of the AgNPs were verified by transmission electron microscopy, TEM (Fig. 1) and found to agree with the manufacturer information (Table 1). The wavelength of the maximum absorbance peak in the UV-Vis spectra also matched the expected values. Regarding the DLS assessment of hydrodynamic diameters (Dh), polydispersity indexes (PdI > 0.3) indicated large variability in particle size, especially for the Cit10 NPs, hence the Z-average sizes may lack accuracy. PEG10 NPs showed higher Dh than Cit10, as expected based on the larger size of PEG compared to citrate. The zeta-potential values confirmed Cit10 AgNPs to have a negative surface charge (ζ -34 mV), which is expected as citrate is using as a coating to prevent agglomeration/aggregation through electrostatic repulsions, whereas PEG10 NPs, which are also designed to stabilize NPs through steric interactions, showed a less negative surface (ζ -14 mV). We have also assessed the amount of ionic silver (Ag^+) released from AgNPs, which was found to be low in water (< 1%), but significantly increased when the NPs were incubated in culture medium. Dissolved Ag^+ reached 14% in Cit10 suspensions after 4 h and 11 % in PEG10 suspensions after 24 and 48 h, this lower value likely relating to a more efficient protection of PEG coating against NP surface oxidation.

Effects on cell growth and viability

HaCaT cells in control conditions (exposed to cell culture medium) showed typical morphology (Figs. 2a and 3a). When cells were exposed to Cit10 and PEG10 AgNPs for 24 h (2b, 2c, 2d and 2e), their confluence decreased, especially at the highest concentration tested (40 µg/mL). The decrease in cell confluence was more visible after 48 h (Fig. 3b, 3c, 3d and 3e). Morphologically, exposed cells (to both Cit10 and PEG10 NPs) showed large precipitates/aggregates of AgNPs in the medium, and confluence appeared to be, on average, lower for Cit10 exposed cells.

The viability of HaCaT cells was negatively affected by both types of AgNP investigated in this study (Fig. 4). Relative to controls, the viability of exposed cells was significantly reduced ($p<0.05$) upon exposure to Cit10 AgNPs at 10 µg/mL and 40 µg/mL after 4 h, 24 h and 48 h. Following PEG10 AgNP exposure, the viability of cells following exposure at a concentration of 10 µg/mL was not affected at 4h but a significant reduction in cell viability was observed at 24 and 48 h at this concentration. At a concentration of 40µg/ml PEG10 NPs significantly decreased cell viability at all time points (4, 24 and 48 h).

NF-κB activation and inflammatory cytokine release

Activation of NF-κB in HaCaT cells by AgNPs was evaluated by immunofluorescence; in its inactive state NF-κB is located in the cytoplasm, and in its active state is localized in the nucleus. Figure 5 a-c shows a positive control with 240 µM of H_2O_2 where there is a great intensity of p65 staining in the nucleus. Also, controls (including: cells only (no staining), cells stained with only the primary antibody and samples stained with the second antibody only) were done to check the autofluorescence in cells (data not shown). In control cells, most NF-κB staining was localized in the cell cytoplasm, with occasional occurrence in the nucleus. Regarding AgNP exposed cells, there was no evidence of NF-κB activation (i.e. no increase in the intensity of staining in the nucelus) (Fig. 5 e-g). A decrease in p65 staining in the nucleus after exposure to 40 µg/mL PEG10 AgNPs was observed comparing to control cells (Fig. 5h). To confirm the decrease in p65 staining observed in Fig. 5h, a quantification of the nucleus fluorescence intensity of HaCaT microscopy images were done using the ImageJ software (Fig. 5i).

The release of cytokines by HaCaT cells treated with AgNPs is shown in Figure 6. Lipopolysaccharide (LPS) stimulated a significant increase in MCP-1 release at 48h, when compared to the control. MCP-1 production significantly decreased following exposure of HaCaT cells to both AgNP types and was most pronounced at a concentration of for 40 µg/mL, compared to negative and positive controls ($p < 0.001$). No effects were observed on the other cytokines studied, IL-1β, IL-6, IL-10 and TNF-α, after exposure to both AgNPs at both times (data not shown).

Discussion

Citrate-coated AgNPs are among the most widely used AgNPs in multiple industrial applications (Tolaymat et al., 2010), while the less used PEG-coated AgNPs have gained increasing attention over recent years by, for instance, the. biomedical industry due to their high stability and reduced reactivity (Brandenberger et al., 2010; Ginn et al., 2014; Ryan et al., 2008; Thorley and Tetley, 2013). Therefore, there is need to better understand the influence of coatings of the biological effects of NPs, and in particular the inflammatory responses. As skin represents one of the major organs in contact with AgNPs, we compared the viability and inflammatory responses induced by citrate or PEG-coated AgNPs with a core diameter of 10 nm (Cit10 and PEG10 AgNPs) in human epidermis keratinocytes (HaCaT cells).

From the cytotoxicity results, Cit10 AgNPs were more toxic than PEG10 NPs. The higher toxicity of Cit10 AgNPs was particularly relevant for low doses, since a lower concentration (10 µg/mL) of Cit0 NPs induced a statistically significant decrease in cell viability 4h post exposure, that was not evident for PEG AgNPs. At higher doses (40 µg/mL) and exposure periods, PEG10 and Cit10 AgNPs reduced viability in similar ways. These data suggest that, for these skin cells, the influence of coating is more important at low AgNP concentrations, whereas by increasing concentration, the influence of coating seems to be less relevant. A significant decrease in BEAS-

2B (bronchial epithelial) cell viability upon exposure to 20 nm citrate-coated AgNPs at 6.25-50 µg/mL after 24 h has been observed previously (Wang et al., 2014). Also, Song et al. (2012) showed a decrease on cell viability in human liver cell line - HL-7702 after exposure to PEG-coated AgNPs in dose- and time-dependent manner at doses from 6.25µg/mL. Future studies could assess the sensitivity of different cell types to the AgNPs used in this study.

A complex interplay between environmental and genetic factors control immune system responses and when a deregulation of immune homeostasis occurs, host defense can be impaired and at the same time cause excessive and potential harmful inflammatory responses, which could be responsible for several immune disorders (Bieber, 2008; Morar et al., 2006). The ability of NPs to elicit pro-inflammatory responses is frequently assessed in *in vitro* and *in vivo* studies as a marker of their toxicity (eg, Schoemaker et al., (2002)). Thus, understanding NP-dependent regulation of cytokine production is essential, since this process conditions shifts from acute to chronic phases of allergic inflammation (Rossi and Zlotnik, 2000). NF-κB pathways have been traditionally associated to increases in the production of inflammatory cytokines which could be implicated in the development of a variety of diseases (Driscoll et al., 1997; Mossman and Churg, 1998). AgNPs did not activate NF-κB in HaCaT cells in this study. In fact, NF-κB may be inhibited after exposure to the higher concentration (40 µg/mL) of PEG10 AgNPs. It is described in literature that the inhibition or absence of NF-κB activation induces apoptosis or sensitizes cells to apoptosis (Schoemaker et al., 2002).

Murray et al (2013) found that a co-exposure of human epidermal keratinocytes (HEK cells) to superparamagnetic iron oxide (SPION) nanoparticles and UVB induced NF-κB activation and release of inflammatory mediators such as the cytokines IL-6 and IL-8. Carbon black NPs have also been demonstrated to induce NF-κB activation in macrophages to stimulate TNFα production (Brown et al., 2004). However, it has also been recognized that NF-κB signaling has important functions in the maintenance of physiological immune homeostasis, particularly in epithelial cells (Wullaert et al., 2011). In a previous work (Bastos et al., 2016), we have demonstrated, by Annexin-V/PI assay and expression of genes involved in apoptosis, that Cit30 AgNPs induced preferably necrotic pathways, while cells exposed to PEG30 AgNPs stimulated increases of cells in earlier phase of apoptosis (therefore a more reversible process) and no necrosis, supporting that coating conditions how these AgNPs influence the cell apoptosis/necrosis pathways. A major role of NF-κB pathways involve the regulation of anti-apoptotic genes, by NF-κB directly binding and inhibiting CASP3, -7 and -9 which seems to be happening in citrate- AgNPs exposed cells (Schoemaker et al., 2002). Considering that only PEG10 AgNPs inhibit NF-κB, we therefore hypothesize that this may be involved in the induction of apoptosis by activating CASP3 found in PEG30-exposed cells versus Cit30-exposed ones. In the future we suggest that NF-κB activation/inhibition may be used to a greater extent when assessing the hazard of coating and AgNPs to better understand the mechanisms (i.e. cellular and molecular events) underlying their

toxicity. On the other hand, Brown et al (2004) showed that ultrafine carbon black particles (UfCB)-induced nuclear translocation of NF-κB in human monocytes which occurs through ROS-mediated mechanism. Indeed, in our previous study 30 nm citrate- and PEG- AgNPs induced a significant increase in the production of ROS by HaCaT cells at the highest dose tested (40 μg/mL), compared to control cells. However, the ROS levels were similar for both NP types which do not explain the NF-κB inhibition by PEG10 AgNPs. Thus, for further studies we also suggest the quantification of NF-κB activation (e.g. by western blotting) and determination of ROS production.

Concerning cytokine release, neither Cit10 nor PEG10 AgNPs induced IL-1β, IL-6, IL-10, TNF-α and MCP-1 production by HaCaT cells. Instead, compared to control cells, they decreased MCP-1 production after 48 h exposure, this reduction being more pronounced at the higher concentration (40 μg/mL), while the control cells presented an increase of this cytokine as already described by Takahashi et al (1995) who reported values close to ours for monocytes and endothelial cells *in vitro*. The information regarding the influence of AgNPs on the stimulation of these cytokines from keratinocytes release is scarce, and sometimes contradictory, as different exposure conditions, concentrations, coating, cell type, NP size and synthesis have been considered in the literature (Abbott Chalew and Schwab, 2013; Giovanni et al., 2015; Miethling-Graff et al., 2014; Orlowski et al., 2013; Samberg et al., 2010; Suliman Y et al., 2013a; Wong et al., 2009; Yen et al., 2009). For instance, Orlowski and co-workers (2013) found an increase of MCP-1 production in murine keratinocytes (murine 291.03C) and by monocytes (RAW 264.7) after exposure to unmodified AgNPs. Also, human umbilical vein endothelial (HUVEC) cells showed a significant increase of IL-6, IL-8 and MCP-1 at doses higher than 1 mg/L AgNPs (Shi et al., 2014). Moreover, confirming the inflammatory potential of AgNPs, several interleukins and TNF-α were reported to increase upon exposure of HEK cells (Samberg et al., 2010) and macrophages (Yen et al., 2010) to AgNPs. On the other hand, several authors reported an undetectable stimulation of cytokines in response to metal NPs, as observed in the present study. For example, Murray et al (2013) demonstrated that HEK cells exposed to superparamagnetic iron oxide nanoparticles maintained the IL-1β, IL-10 and TNF-α below detectable levels (while increasing IL-6); and also that mouse epidermal cells (JB6 P+) maintained INF-γ and IL-12 below the detectable levels after exposure to the same nanoparticles. Similarly, Samberg et al (2010) did not find detectable levels of IL-10 in HEK cells exposed to unwashed AgNPs. In mice peritoneal tissues and in RAW cells, Wong et al (2009) demonstrated that AgNPs have an anti-inflammatory effect decreasing TNF-α, and INF-γ. Also, Parnsamut and Brimson (2015) found that AgNPs inhibited TNF-α expression in leukemic cell lines. It is known that cytokines can adsorb onto the surface of particles, which may compromise their detection (Brown et al., 2010). Thus, it should not be excluded that AgNPs may induce cytokine production by keratinocytes but that the cytokines bind to the AgNP surface to prevent their detection. How proteins bind to nanoparticles

is currently an important topic of debate. For example, Deng et al (2013) showed that human plasma proteins differently bind to positively and negatively charged polymer-coated gold NPs, which elicited different biological responses, and that only the negatively charged nanoparticles induced cytokine release from THP-1 cells. While proteins can bind to different nanoparticles, the biological outcome may not be the same. Selection of cytokines for assessment in this study was prioritized based on the outcome of a literature search which identified cytokines that are commonly produced following exposure of cells to NPs. Future studies could therefore assess a wider panel of cytokines.

In summary, our study demonstrated that while citrate- and PEG-coated AgNPs decreased the viability of HaCaT cells. Citrate coated AgNPs were more cytotoxic than PEG coated NPs, particularly at low concentrations and shorter incubation times. At higher AgNPs concentration, the influence of coating became less relevant. Also, we demonstrated that, independent of the coating, AgNPs did not induce cytokine production, and decreased MCP-1 release. Finally, PEG10 AgNPs at high concentrations inactivated the transcription factor NF-κB, and putative correlation with anti-inflammatory and anti-apoptotic homeostasis should be further explored.

Competing interests

The authors declare that they have no competing interests.

Acknowledgments

This work was developed in the scope of the projects CICECO-Aveiro Institute of Materials (Ref. FCT UID/CTM/50011/2013) and CESAM (Ref. FCT UID/AMB/50017/2013), financed by national funds through the FCT/MEC and when applicable co-financed by the European Regional Development Fund (FEDER) under the PT2020 Partnership Agreement. Funding to the project FCOMP-01-0124-FEDER-021456 (Ref. FCT PTDC/SAU-TOX/120953/2010) by FEDER through COMPETE and by national funds through FCT, and the FCT-awarded grants (SFRH/BD/81792/2011; SFRH/BPD/111736/2015) are acknowledged. I.F.D and A.L.D.S. acknowledge FCT/MCTES for the research contracts under the Program 'Investigador FCT' 2014.

374 **References**

375 Abbott Chalew TE, Schwab KJ (2013) Toxicity of commercially available engineered
376 nanoparticles to Caco-2 and SW480 human intestinal epithelial cells. Cell Biol Toxicol
377 29(2):101-116.
378 Abdelhalim MAK, Jarrar BM (2011) Renal tissue alterations were size-dependent with smaller
379 ones induced more effects and related with time exposure of gold nanoparticles. Lipids Health
380 Dis 10(1):1.
381 Ahlberg S, Meinke MC, Werner L, Epple M, Diendorf J, Blume-Peytavi U, Lademann J, Vogt A,
382 Rancan F (2014) Comparison of silver nanoparticles stored under air or argon with respect to
383 the induction of intracellular free radicals and toxic effects toward keratinocytes. Eur J Pharm
384 Biopharm 88(3):651-657
385 Bastos V, de Oliveira JF, Brown D, Jonhston H, Malheiro E, Daniel-da-Silva AL, Duarte IF,
386 Santos C, Oliveira H (2016) The influence of Citrate or PEG coating on silver nanoparticle
387 toxicity to a human keratinocyte cell line. Toxicol Lett 249:29-41.
388 Behra R, Sigg L, Clift M, Herzog F, Minghetti M, Johnston B, Petri-Fink A, Rothen-Rutishauser
389 B (2013) Bioavailability of silver nanoparticles and ions: from a chemical and biochemical
390 perspective. J R Soc Interface 10(87):20130396.
391 Benn T, Westerhoff P (2008) Nanoparticle silver released into water from commercially available
392 sock fabrics. Environ Sci Technol 42(11):4133-4139 .
393 Bieber T (2008) Atopic dermatitis. N Engl J Med 358 (14):1483-1494.
394 Boonkaew B, Kempf M, Kimble R, Cuttle L (2014) Cytotoxicity testing of silver-containing burn
395 treatments using primary and immortal skin cells. Burns 40(8):1562-1569.
396 Brandenberger C, Mühlfeld C, Ali Z, Lenz A-GG, Schmid O, Parak WJ, Gehr P, Rothen-
397 Rutishauser B (2010) Quantitative evaluation of cellular uptake and trafficking of plain and
398 polyethylene glycol-coated gold nanoparticles. Small 6(15):1669-1678.
399 Brown DM, Dickson C, Duncan P, Al-Attili F. Stone V (2010) Interaction between nanoparticles
400 and cytokine proteins: impact on protein and particle functionality. Nanotechnology
401 21(21):215104.
402 Brown DM, Donaldson K, Borm PJ, Schins RP, Dehnhardt M, Gilmour P, Jimenez LA, Stone V
403 (2004) Calcium and ROS-mediated activation of transcription factors and TNF-alpha cytokine
404 gene expression in macrophages exposed to ultrafine particles. Am J Physiol Lung Cell Mol
405 Physiol 286(2):L344-L353.
406 Caballero-Díaz E, Pfeiffer C, Kastl L, Gil P, Simonet B, Valcárcel M, Lamana J, Laborda F, Parak
407 WJ (2013) The toxicity of silver nanoparticles depends on their uptake by cells and thus on
408 their surface chemistry. Part Part Syst Charact 30(12):1079-1085.

409 Comfort KK, Maurer EI, Hussain SM, (2014) Slow release of ions from internalized silver
410 nanoparticles modifies the epidermal growth factor signaling response.
411 Colloids Surf B Biointerfaces 123:136-142.
412 Deng ZJ, Liang M, Toth I, Monteiro M, Minchin RF (2013) Plasma protein binding of positively
413 and negatively charged polymer-coated gold nanoparticles elicits different biological
414 responses. Nanotoxicology 7(3):314-322.
415 Driscoll KE, Carter JM, Hassenbein DG (1997) Cytokines and particle-induced inflammatory cell
416 recruitment. Environ Health Perspect 105(Suppl 5):1159.
417 Eckhardt S, Brunetto P, Gagnon J, Priebe M, Giese B, Fromm K (2013) Nanobio silver: its
418 interactions with peptides and bacteria, and its uses in medicine. Chem Rev 113(7):4708-4754.
419 EPA, EPA (2010) State of the Science Literature Review: Everything Nanosilver and More.
420 Scientific, Technical, Research, Engineering and Modeling Support Final Report.
421 Fujiwara N, Kobayashi K (2005) Macrophages in inflammation.
422 Curr Drug Targets Inflamm Allergy 4(3):281-286.
423 George R, Merten S, Wang TT, Kennedy P, Maitz P (2014) In vivo analysis of dermal and
424 systemic absorption of silver nanoparticles through healthy human skin. Australas J Dermatol
425 55(3):185-190.
426 Ginn C, Khalili H, Lever R, Brocchini S (2014) PEGylation and its impact on the design of new
427 protein-based medicines. Future Med Chem 6(16):1829-1846.
428 Giovanni M, Yue J, Zhang L, Xie J, Ong CN (2015) Pro-Inflammatory Responses of RAW264. 7
429 Macrophages when Treated with Ultralow Concentrations of Silver, Titanium Dioxide, and
430 Zinc Oxide Nanoparticles. J Hazard Mater 297:146-152.
431 Graves JD, Craxton A, Clark EA (2004) Modulation and function of caspase pathways in B
432 lymphocytes. Immunol Rev 197(1):129-146.
433 Kelso A (1998) Cytokines: principles and prospects. Immunol Cell Biol 76(4), 300-317.
434 Kim TH, Kim M, Park HS, Shin US, Gong MS, Kim HW (2012) Size-dependent cellular toxicity
435 of silver nanoparticles. J Biomed Mater Res A 100(4):1033-1043.
436 Larese FF, D'Agostin F, Crosera M, Adami G, Renzi N, Bovenzi M, Maina G (2009) Human skin
437 penetration of silver nanoparticles through intact and damaged skin. Toxicology 255(1):33-37.
438 Lu W, Senapati D, Wang S, Tovmachenko O, Singh A, Yu H, Ray P (2010) Effect of Surface
439 Coating on the Toxicity of Silver Nanomaterials on Human Skin Keratinocytes. Chem Phys
440 Lett 487(1):92-96.
441 Miethling-Graff R, Rumpker R, Richter M, Verano-Braga T, Kjeldsen F, Brewer J, Hoyland J,
442 Rubahn H-GG, Erdmann H (2014) Exposure to silver nanoparticles induces size- and dose-
443 dependent oxidative stress and cytotoxicity in human colon carcinoma cells. Toxicol In
444 Vitro 28(7):1280-1289.

445 Morar N, Willis-Owen SAG, Moffatt MF (2006) The genetics of atopic dermatitis. J Allergy Clin
446 Immun 118(1):24-34.
447 Mossman BT, Churg A (1998) Mechanisms in the pathogenesis of asbestosis and silicosis. Am J
448 Respir Crit Care Med 157(5):1666-1680.
449 Murray AR, Kisin E, Inman A, Young S-H, Muhammed M, Burks T, Uheida A, Tkach A, Waltz
450 M, Castranova V (2013) Oxidative stress and dermal toxicity of iron oxide nanoparticles in
451 vitro. Cell Biochem Biophys 67(2):461-476.
452 Noursadeghi M, Tsang J, Haustein T, Miller RF, Chain BM, Katz DR (2008) Quantitative imaging
453 assay for NF-kappaB nuclear translocation in primary human macrophages. J
454 Immunol Methods 329(1):194-200.
455 Nowack B, Bucheli T (2007) Occurrence, behavior and effects of nanoparticles in the
456 environment. Environ Pollut 150(1):5-22.
457 Nowack B, Krug H, Height M (2011) 120 years of nanosilver history: implications for policy
458 makers. Environ Sci Technol 45(4):1177-1183.
459 Orlowski P, Krzyzowska M, Zdanowski R, Winnicka A, Nowakowska J, Stankiewicz W,
460 Tomaszewska E, Celichowski G, Grobelny J (2013) Assessment of in vitro cellular responses
461 of monocytes and keratinocytes to tannic acid modified silver nanoparticles. Toxicol in
462 Vitro 27(6):1798-1808.
463 Pang C, Brunelli A, Zhu C, Hristozov D, Liu Y, Semenzin E, Wang W, Tao W, Liang J, Marcomini
464 A, et al (2015) Demonstrating approaches to chemically modify the surface of Ag nanoparticles
465 in order to influence their cytotoxicity and biodistribution after single dose acute intravenous
466 administration. Nanotoxicology 1-11.
467 Park E-JJ, Choi K, Park K (2011a) Induction of inflammatory responses and gene expression by
468 intratracheal instillation of silver nanoparticles in mice. Arch Pharm Res 34(2):299-307.
469 Park J, Lim D-HH, Lim H-JJ, Kwon T, Choi J-sS, Jeong S, Choi I-HH, Cheon J (2011b) Size
470 dependent macrophage responses and toxicological effects of Ag nanoparticles. Chem
471 Commun (Camb) 47(15):4382-4384.
472 Parnsamut C, Brimson S (2015) Effects of silver nanoparticles and gold nanoparticles on IL-2, IL-
473 6, and TNF-α production via MAPK pathway in leukemic cell lines. Genet Mol
474 Res 14(2):3650.
475 Rossi D, Zlotnik A (2000) The biology of chemokines and their receptors. Annu Rev
476 Immunol 18(1):217-242.
477 Ryan SMM, Mantovani G, Wang X, Haddleton DM, Brayden DJ (2008) Advances in PEGylation
478 of important biotech molecules: delivery aspects. Expert Opin Drug Deliv 5(4):371-383.
479 Samberg ME, Oldenburg SJ, Monteiro-Riviere NA (2010) Evaluation of Silver Nanoparticle
480 Toxicity in Skin in Vivo and Keratinocytes in Vitro. Environ Health Perspect 118(3):407.

Schinwald A, Murphy F, Prina-Mello A, Poland C, Byrne F, Movia D, Glass J, Dickerson JC, Schultz DA, Jeffree CE, Macnee W, Donaldson K (2012) The threshold length for fibre-induced acute pleural inflammation: shedding light on the early events in asbestos-induced mesothelioma. Toxicol Sci 128(2):461-70.

Schoemaker MH, Ros JE, Homan M, Trautwein C (2002) Cytokine regulation of pro-and anti-apoptotic genes in rat hepatocytes: NF-κB-regulated inhibitor of apoptosis protein 2 (cIAP2) prevents apoptosis. J Hepatol 36(6):742-750.

Sharma V, Yngard R, Lin Y (2009) Silver nanoparticles: green synthesis and their antimicrobial activities. Adv Colloid Interface Sci 145(1):83-96.

Shi J, Sun X, Lin Y, Zou X, Li Z, Liao Y, Du M, Zhang H (2014) Endothelial cell injury and dysfunction induced by silver nanoparticles through oxidative stress via IKK/NF-κB pathways. Biomaterials 35(24):6657-6666.

Suliman YA, Ali D, Alarifi S, Harrath A, Mansour L, Alwasel S (2013a) Evaluation of cytotoxic, oxidative stress, proinflammatory and genotoxic effect of silver nanoparticles in human lung epithelial cells. Environ Toxicol 30(2):149-160.

Suliman YAO, Ali D, Alarifi S, Harrath AH, Mansour L, Alwasel SH (2013b) Evaluation of cytotoxic, oxidative stress, proinflammatory and genotoxic effect of silver nanoparticles in human lung epithelial cells. Environ Toxicol 30(2):149-160.

Takahashi M, Masuyama JI, Ikeda U, Kasahara T, Kitagawa SI, Takahashi YI, Shimada K, Kano S (1995) Induction of monocyte chemoattractant protein-1 synthesis in human monocytes during transendothelial migration in vitro. Circ Res 76(5):750-757.

Tejamaya M, Römer I, Merrifield R, Lead J (2012) Stability of citrate, PVP, and PEG coated silver nanoparticles in ecotoxicology media. Environ Sci Technol 46(13), 7011-7017.

Thorley AJ, Tetley TD (2013) New perspectives in nanomedicine. Pharmacol Therapeut 140(2):176-185.

Tolaymat TM, El Badawy AM, Genaidy A, Scheckel KG, Luxton TP, Suidan M (2010) An evidence-based environmental perspective of manufactured silver nanoparticle in syntheses and applications: a systematic review and critical appraisal of peer-reviewed scientific papers. Sci Total Environ 408(5):999-1006.

Twentyman P, Luscombe M (1987) A study of some variables in a tetrazolium dye (MTT) based assay for cell growth and chemosensitivity. Br J Cancer 56(3):279.

Vance ME, Kuiken T, Vejerano EP, McGinnis SP, Hochella Jr MF, Rejeski D, Hull, MS (2015) Nanotechnology in the real world: Redeveloping the nanomaterial consumer products inventory. Beilstein J Nanotechnol 6(1):1769-1780.

Wang X, Ji Z, Chang C, Zhang H, Wang M, Liao Y-P, Lin S, Meng H, Li R, Sun B, et al (2014) Use of coated silver nanoparticles to understand the relationship of particle dissolution and bioavailability to cell and lung toxicological potential. Small 10(2):385-398.

Wong KK, Cheung SO, Huang L, Niu J, Tao C, Ho C-MM, Che C-MM, Tam PK (2009) Further evidence of the anti-inflammatory effects of silver nanoparticles. ChemMedChem 4(7):1129-1135.

Wullaert A, Bonnet MC, Pasparakis M (2011) NF-κB in the regulation of epithelial homeostasis and inflammation. Cell Res 21(1):146-158.

Yang E-JJ, Jang J, Lim D-HH, Choi I-HH (2012) Enzyme-linked immunosorbent assay of IL-8 production in response to silver nanoparticles. Methods Mol Biol 131-139.

Yarilin AA, Belyakov IM (2004) Cytokines in the thymus: production and biological effects. Curr Med Chem 11(4):447-464.

Yen H-J, Hsu S-H, Tsai C-L (2009) Cytotoxicity and immunological response of gold and silver nanoparticles of different sizes. Small 5(13):1553-1561.

Yoshizumi M, Nakamura T, Kato M, Ishioka T, Kozawa K, Wakamatsu K, Kimura H (2008) Release of cytokines/chemokines and cell death in UVB-irradiated human keratinocytes, HaCaT. Cell Biol Int 32(11):1405-1411.

Zhang LW, Yu WW, Colvin VL, Monteiro-Riviere NA (2008) Biological interactions of quantum dot nanoparticles in skin and in human epidermal keratinocytes. Toxicol Appl Pharmacol 228(2):200-211.

Fig. 1 Transmission electron microscopy (TEM) images of Cit10 and PEG10 AgNPs used in this work

Fig. 2 Light microscopy images (100X) of HaCaT cells exposed to 10 nm citrate- AgNPs or PEG-AgNPs (Cit10 or PEG10) for 24 h. a) 0 (control); b) Cit10, 10 µg/mL; c) Cit10, 40 µg/mL; d) PEG10, 10 µg/mL; and e) PEG10, 40 µg/mL. Bar corresponds to 100 µm

Fig. 3 Light microscopy images (100X) of HaCaT cells exposed to 10 nm citrate- AgNPs or PEG-AgNPs (Cit10 or PEG10) for 48 h. a) 0 (control); b) Cit10, 10 µg/mL; c) Cit10, 40 µg/mL; d) PEG10, 10 µg/mL; and e) PEG10, 40 µg/mL. Bar corresponds to 100 µm

Fig. 4 Relative cell viability (%) of HaCaT cells after exposure to 10 and 40 µg/mL of 10 nm citrate- AgNPs or PEG- AgNPs (Cit10 or PEG10), measured by MTT assay, at 4, 24 and 48 h post exposure. Data expressed as mean and standard deviation (n = 3). * indicate significant differences between control at $p < 0.05$

Fig. 5 Microscopy images of HaCaT cells. a) - c) are fluorescence microscopy images (400X) of immunofluorescence of HaCaT cells treated with anti NF-kB p65 antibody after stimulation with 240 µM H_2O_2 for 10 min prior fixation: a) p65 subunit of NF-kB (alexa fluor 488 anti-rabbit IgG);

b) DAPI staining the nucleus; c) Overlap of a and b images. d) - h) are confocal microscopy images of immunofluorescence of p65 subunits of NF-kB in human HaCaT keratinocytes exposed to AgNPs for 4 h: d) 0 (control); e) 10 µg/mL of Cit10; f) 40 µg/mL of Cit10; g) 10 µg/mL of PEG10; h) 40 µg/mL of PEG10. Bar corresponds to 100 µm. i) is the quantification of the nucleus fluorescence intensity of HaCaT microscopy images presented in Fig.4h using the ImageJ software. Data expressed the mean and standard deviation. ** indicate significant differences between control at $p < 0.01$

Fig. 6 Cytokine release by HaCaT cells after 24 and 48h exposure to 10 nm citrate- or PEG-AgNPs (Cit10 or PEG10). Control + is a positive control by adding LPS to cells. Data represent the mean ± standard deviation (n = 3) of the concentration (pg /ml) of MCP-1 cytokine released from the cells after NPs treatment

571

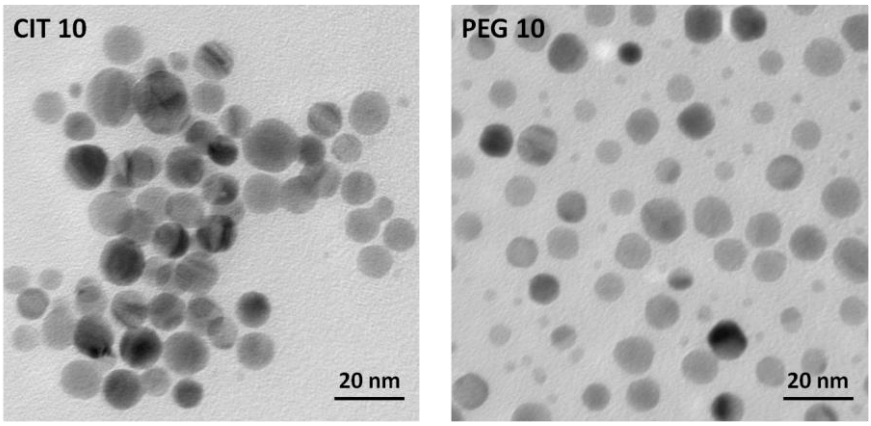

Figure 1

572

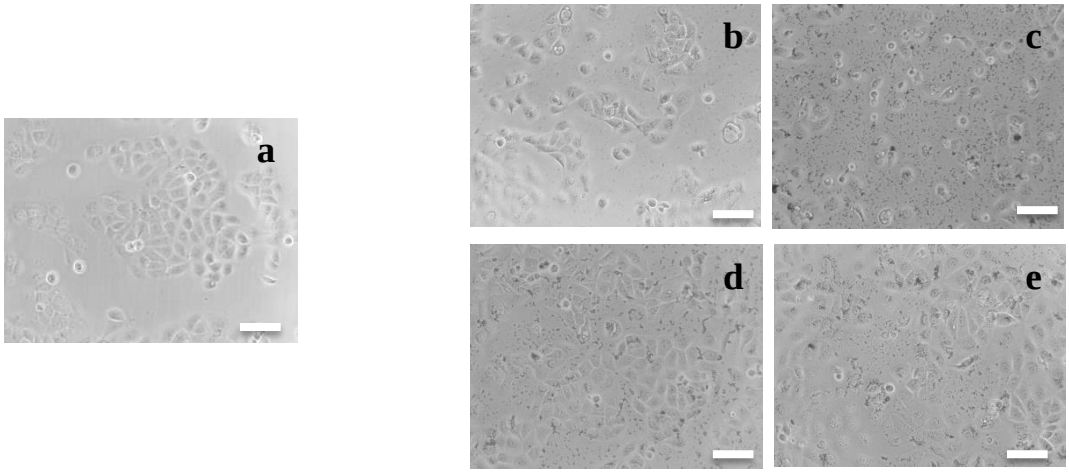

Figure 2

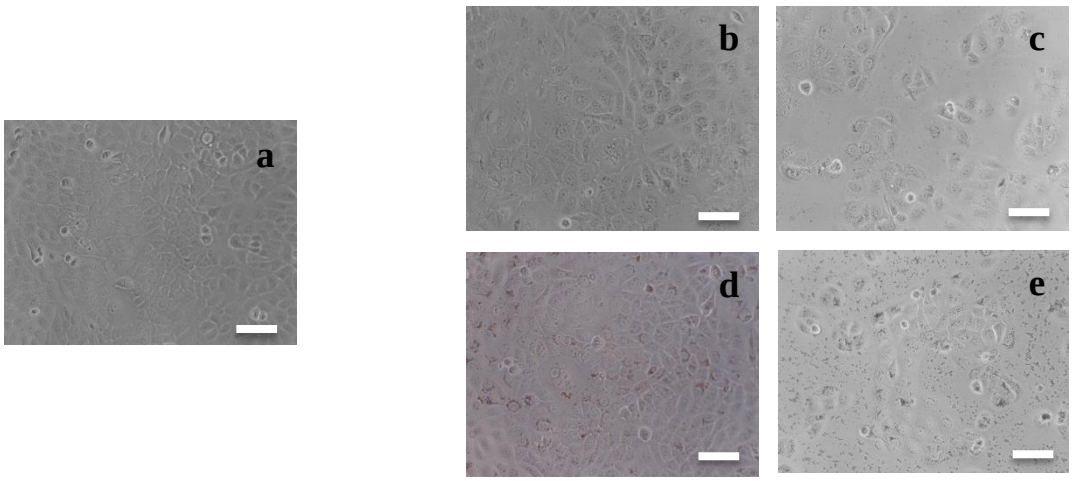

Figure 3

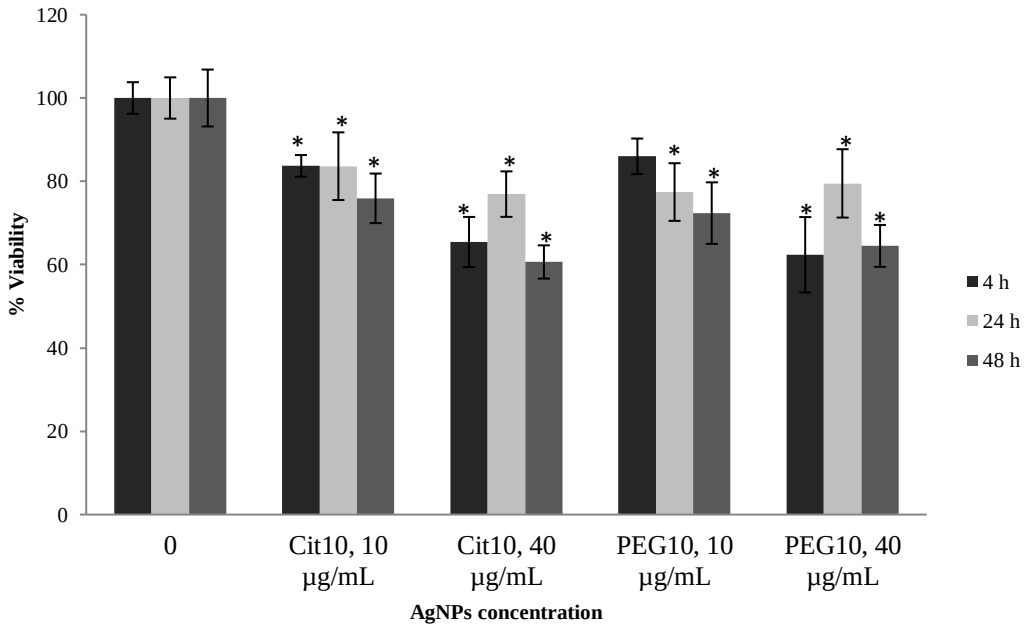
120
100
80
60
40
20
0
% Viability
*
0
Cit10, 10 µg/mL
Cit10, 40 µg/mL
PEG10, 10 µg/mL
PEG10, 40 µg/mL
AgNPs concentration
4 h
24 h
48 h

Figure 4

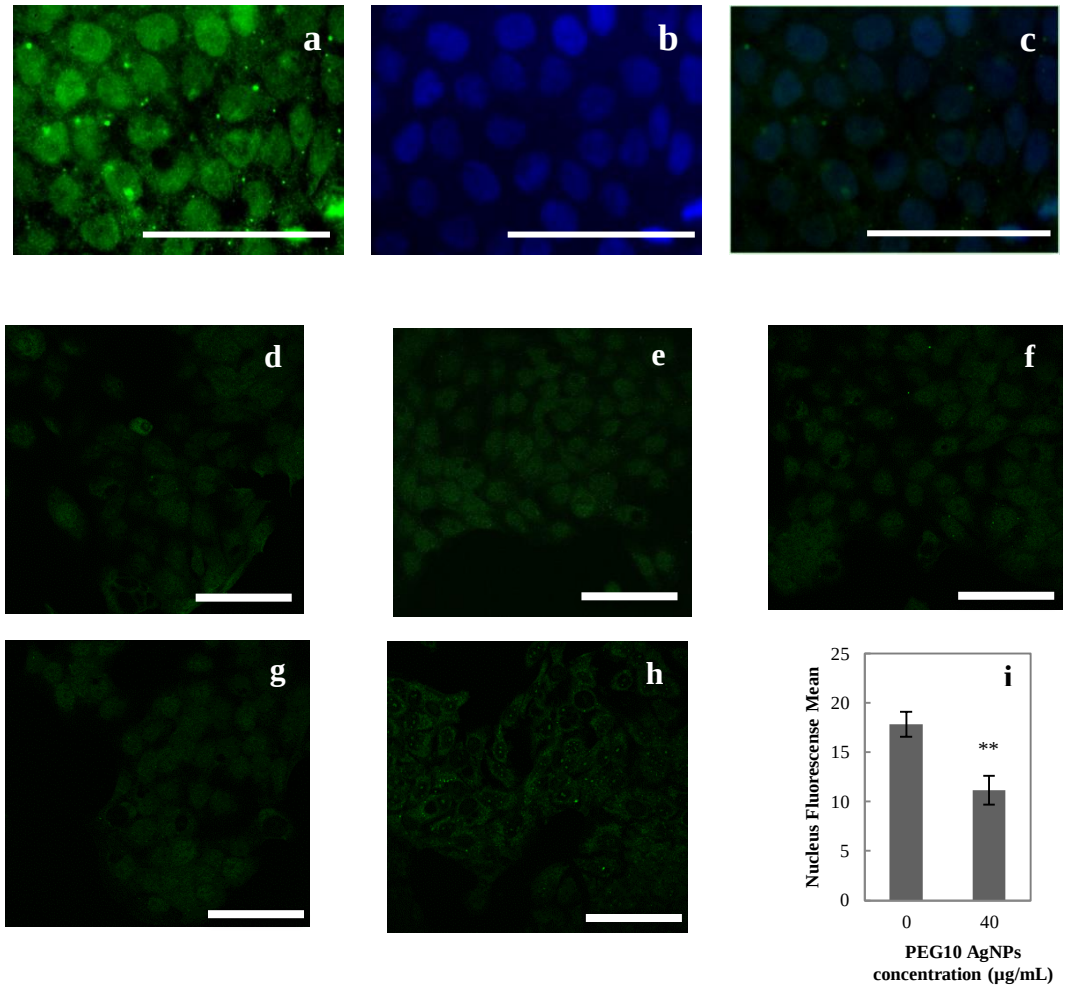
a
b
c
d
e
f
g
h
i
Nucleus Fluorescense Mean
25
20
15
10
5
0
**
0
40
PEG10 AgNPs
concentration (µg/mL)

Figure 5

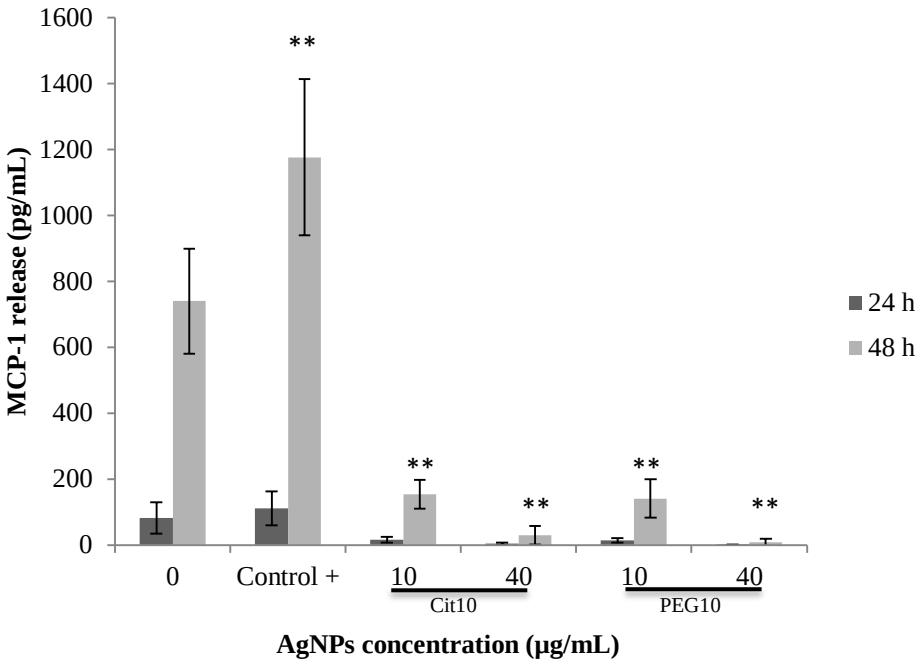
1600
1400
1200
1000
800
600
400
200
0
MCP-1 release (pg/mL)
**
**
**
**
**
24 h
48 h
0
Control +
10
40
10
40
Cit10
PEG10
AgNPs concentration (µg/mL)

Figure 6